Geophys. J. Int. (1994) **118,** 245–254

Efficient calculation of complete differential seismograms for laterally homogeneous earth models

George E. Randall
Department of Geological Sciences, University of South Carolina, Columbia, SC 29208, USA

Accepted 1993 October 10. Received 1993 August 19; in original form 1993 January 11

SUMMARY

Differential seismograms, the sensitivity of the seismogram to perturbations of parameters of the earth model, are essential for waveform modelling with iterative non-linear optimization techniques. The growing number of broad-band high-dynamic-range fixed and portable stations provide a rich data set of regional distance events with accurate locations and source mechanisms that are ideal for modelling lithospheric structure. An efficient technique for calculating differential seismograms for complete synthetic seismograms in laterally homogeneous earth models will significantly decrease the computational burden of seismic-waveform inverse modelling. The technique we present here is equivalent to computing three synthetic seismograms in multilayered models, contrasted with $N+1$ seismograms for a typical brute-force approach, which reduces the work to $3/(N+1)$ or about a 90 per cent saving for 30 layers. The lateral-homogeneity requirement will yield path-averaged structures which may form the basis for later tomographic studies to resolve lateral variations.

Key words: earth models, synthetic seismograms, waveform analysis.

1 INTRODUCTION

Two important developments in seismology in the late 1960's and early 1970's were the development of linear-inverse theory (e.g. Backus & Gilbert 1967, 1968; Franklin 1970; Jackson 1972) and the development of techniques for computing accurate synthetic seismograms for detailed, plane-layered earth models (e.g. Helmberger 1968; Fuchs & Muller 1971; Kennett 1974). Since then, the application of systematic waveform matching using inverse theory has led to a significant advancement of our knowledge of gross earth structure and our ability to estimate earthquake mechanisms. Of particular interest in this work are seismic methods that utilize waveforms to estimate the gross properties of the earth either jointly with the seismic source or independently of the earthquake mechanism. Specifically, we address problems for which the earth is parametrized as a laterally homogeneous medium. Although recent trends in earth modelling are aimed at delineating lateral-velocity variations, robust first-order estimates of the structure are often critical to these efforts, since most approaches solve for small perturbations to a simpler, and often 1-D, starting model.

A key step in the application of inverse theory to waveform modelling is the computation of linearized sensitivities of the seismogram to the model parameters. For specific cases, approximate partial derivatives of the seismogram with respect to the model parameters can be computed quickly (Mellman 1980; Shaw & Orcutt 1985) but for general, complete responses, the numerical demands remain significant. A technique for computing differential seismograms using locked modes (Gomberg & Masters 1988) shows promise for fundamental and higher modes, but for complete synthetics in regions where attenuation varies strongly with depth, locked modes synthetics with perturbations for attenuation (Day *et al.* 1989) can significantly misrepresent portions of the complete waveform. In this paper we present a method to rapidly compute differential seismograms for point-source seismograms in laterally homogeneous earth structures. This approach significantly decreases the time necessary to estimate the gross characteristics of earth structure using seismic waveforms. The increased efficiency of inverse modelling will make it practical to investigate problems such as the dependence of the inversion results on the initial model by performing numerous inversions using a suite of initial models.

Our technique is based on the reflection-matrix method developed by Kennett (1974), Kennett & Kerry (1979), and Kennett (1980) and summarized in Kennett (1983). In Kennett's approach, the wave equation for a general, point-moment tensor or point-force source in a laterally

homogeneous media is solved in the frequency-slowness domain for a range of frequencies and slownesses. To compute the time-domain response an integration is performed over slowness, and the resulting spectrum is transformed to the time domain. In the interest of space, we omit a general review of the computation of synthetic seismograms using this approach and refer the reader to Kennett (1983) for a detailed background, and Chapman & Orcutt (1985) for a general perspective on Kennett's method. Information on efficient numerical algorithms (Phinney, Odom & Fryer 1987) and guidelines for choosing sensible values for the parameters affecting the accuracy of the synthetics (Mallick & Frazer 1987) exist in the literature. The purpose of this note is to present an efficient algorithm for the computation of differential seismograms. Our description of the algorithm relies on some details of Kennett's approach and we review them in the next section. We follow with the description of the algorithm for computing the differential seismograms. Our approach is quite efficient and can compute the sensitivities for a model with N layers in roughly the time it takes to compute three complete responses.

2 FORMULATION

We consider the seismic response of azimuthally variable sources such as moment tensors and point forces in a plane-layered earth model and so adopt a cylindrical coordinate system as a natural-reference frame. The top of the model is the free surface and the bottom is a uniform half-space. In the model, stress and displacement are continuous at the interfaces between layers, and the source is characterized by a discontinuity in stress and displacement. Anelastic attenuation is simulated by employing complex compressional and shear-wave velocities. The equations of motion are Hankel transformed over the range, r, and Fourier transformed over time, t. The result is a set of coupled, second-order ordinary differential equations in depth, z. Vanishing traction at the free surface and radiation boundary conditions at the bottom of the layered velocity model complete the system. The transformed equations are solved for a range of temporal frequencies and horizontal slownesses, and then inverse transformed back to the time and space domain. The inverse transform over slowness is performed using numerical integration and an inverse Fourier transform is used to calculate the time-domain synthetic seismograms. The synthesis integrals over frequency and slowness (the inverse Fourier and Hankel transforms) described in Kennett (1983) eqs 7.57P and 7.57H are presented here in expanded form, neglecting near-field terms and higher order angular terms, as

$$u_z(r, \phi, t) = \frac{1}{2\pi}\int_{-\infty}^{\infty} d\omega \times \exp(-i\omega t)\omega^2 \int_0^{\infty} dpp \sum_{m=-2}^{+2} u_z(p, m, \omega) J_m(\omega pr) \times \exp(im\phi) \quad (1v)$$

$$u_r(r, \phi, t) = \frac{1}{2\pi}\int_{-\infty}^{\infty} d\omega \times \exp(-i\omega t)\omega^2 \int_0^{\infty} dpp \sum_{m=-2}^{+2} u_r(p, m, \omega) J_{m-1}(\omega pr \times \exp(im\phi) \quad (1r$$

$$u_t(r, \phi, t) = \frac{1}{2\pi}\int_{-\infty}^{\infty} d\omega \times \exp(-i\omega t)\omega^2 \int_0^{\infty} dpp \sum_{m=-2}^{+2} -u_t(p, m, \omega) J_{m-1}(\omega pr \times \exp(im\phi) \quad (1t$$

u_z, u_r and u_t are the vertical, radial and tangentia components of displacement. The azimuth of the receiver i ϕ and m is the angular order of the source. The radia frequency is ω and the slowness, or reciprocal of phas velocity is p.

The transformed displacements, u_z, u_r, and u_t, are th solution of a second-order ordinary differential equation ir the depth with the boundary conditions and excitation Using the method of Kennett (1983), the P–SV displacement in the vertical and radial directions at the free surface of a half-space of N layers with a source at depth z_s are obtained using Kennett (7.36)

$$\begin{bmatrix} u_z(\omega, p, m) \\ u_r(\omega, p, m) \end{bmatrix} = \mathbf{w}_0(\omega, p, m) = \tilde{\mathbf{W}}[\mathbf{I} - \mathbf{R}_D^{0S}\tilde{\mathbf{R}}]^{-1}\mathbf{T}_U^{0S}[\mathbf{I} - \mathbf{R}_D^{SN}\mathbf{R}_U^{fS}]^{-1}\mathbf{v}_U(z_s, \omega, p, m). \quad (2)$$

The excitation vector, $\mathbf{v}_U(z_s, \omega, p, m)$ and displacement vector, $\mathbf{w}_0(\omega, p, m)$ vectors are of order 2. Terms represented by boldface upper case characters are the two-by-two reflection $\mathbf{R}$, transmission $\mathbf{T}$ and displacement $\mathbf{W}$ matrices. The tangential motions are described by an equivalent scalar equation.

Expression (2) can be analysed by studying major groups of terms working from right to left. The excitation vector, $\mathbf{v}_U(z_s, \omega, p, m)$ contains the net upward radiation, the direct upward radiation from the source, plus the reflected waves initially radiated downward from the source

$$\mathbf{v}_U(z_s, \omega, p, m) = [\Sigma_U(z_s, \omega, p, m) + \mathbf{R}_D^{SN}\Sigma_D(z_s, \omega, p, m)] \quad (3)$$

where the source terms $\Sigma_U(z_s, \omega, p, m)$, $\Sigma_D(z_s, \omega, p, m)$ are vectors of compressional and shear-wave amplitudes, generated by a discontinuity in stress and displacement. We can compute the discontinuity in stress and displacement for the desired moment tensor or point-force source using the representation theorem and the velocity and density parameters of the medium at the source depth. Although the medium is isotropic, the source terms are not, and they require a periodic, azimuthal expansion. Fortunately, moment tensors and point forces only require simple azimuthal expansion with terms of orders 0, ±1, and ±2, depending on the particular source-moment-tensor term or point-force term. The key results are described in Kennett (1983) eqs 4.59, 4.60 and 4.63. The azimuthal terms are only a function of the source and not the medium response, and not all sources excite all the azimuthal terms. Careful coding

for the source excitation that exploits the source azimuthal dependence can minimize the computation load.

The next major term in the response (2) (reading from right to left) is the reverberation operator for the entire structure,

$$[\mathbf{I} - \mathbf{R}_D^{SN}\mathbf{R}_U^{fS}]^{-1}. \tag{4}$$

Here this operator has been expressed using waves which start propagating upward at the source level z_s, and finish complete reverberations through the entire structure as waves, again propagating upward at the source level. The reflection matrices $\mathbf{R}_D^{SN}$ and $\mathbf{R}_U^{fS}$ represent the reflection of downward travelling waves from the layering or beneath z_s bounded below by the half-space and the reflection of upward travelling waves for the layering above z_s bounded above by the free surface. The matrix inversion will fail if the expression inside the brackets is singular, but for attenuating media the singularities will not lie on the real p axis, and so will not adversely affect the integrand.

The next and final operator contributes the response of the region between the source depth and the free surface,

$$\tilde{\mathbf{W}}[\mathbf{I} - \mathbf{R}_D^{0S}\tilde{\mathbf{R}}]^{-1}\mathbf{T}_U^{0S} \tag{5}$$

to upward-travelling waves at the source depth z_s. The synthesis of this operator has been studied (Randall 1989) for the analysis of teleseismic waveforms and receiver-function modelling. This term represents, from right to left, the transmission of waves from the source depth to the free surface, reverberations within the structure between the source depth and the free surface, and finally transformation from P and SV waves to vertical and radial displacements at the free surface using the operator $\tilde{\mathbf{W}}$.

If the complete expression for the displacements is reformulated by associating the reflection matrix in the source term for downward-radiated energy with the other medium response terms, the response of the medium to either upgoing

$$\tilde{\mathbf{W}}[\mathbf{I} - \mathbf{R}_D^{0S}\tilde{\mathbf{R}}]^{-1}\mathbf{T}_U^{0S}[\mathbf{I} - \mathbf{R}_D^{SN}\mathbf{R}_U^{fS}]^{-1} \tag{6}$$

or downgoing waves

$$\tilde{\mathbf{W}}[\mathbf{I} - \mathbf{R}_D^{0S}\tilde{\mathbf{R}}]^{-1}\mathbf{T}_U^{0S}[\mathbf{I} - \mathbf{R}_D^{SN}\mathbf{R}_U^{fS}]^{-1}\mathbf{R}_D^{SN} \tag{7}$$

can be simply calculated. With this minor revision, it is possible to calculate the response to several different sources rapidly, using a single medium-response calculation.

All of the reflection and transmission matrices are calculated recursively using simple reflection and transmission matrices for each individual interface and recursion relation which define the reverberation within layers. The interface reflection and transmission matrices are treated as being independent of frequency since they only depend weakly on the frequency through the frequency dependence of complex velocity parameters used to describe the attenuation. For teleseismic distances, accurate modelling of turning rays will require a frequency-dependent calculation for the interface matrices. This will require additional computation and storage, but will not substantially complicate the code.

3 EFFICIENT METHODS FOR DIFFERENTIAL SEISMOGRAMS

Differential seismograms are most commonly used in inverse problems in which a set of seismograms are inverted to estimate the properties of the earth. The relationship between the model and the seismogram is non-linear and a solution is often obtained using an iterative sequence of linearizations. The non-linear relationship between the model parameters and the seismograms is approximated using a first-order Taylor series

$$\{S_{obs}(t) - S_{syn}[t, \alpha(z)]\} \approx \frac{\partial S_{syn}[t, \alpha(z)]}{\partial \alpha(z)} \Delta\alpha(z). \tag{8}$$

In this expansion, $S_{obs}(t)$ is the vector of time samples of the observed seismogram, and $S_{syn}[t, \alpha(z)]$ is the vector of time samples of the synthetic seismogram for a reference velocity model, $\alpha(z)$. The left-hand side of (8) is a residual vector, the difference between the observed seismogram and the computed seismogram. The differential seismograms,

$$\frac{\partial S_{syn}[t, \alpha(z)]}{\partial \alpha(z)} \tag{9}$$

form a matrix which represents the differential change in the vector of seismogram time samples for a differential change of each model parameter, or the sensitivity of the seismogram to the parameters in the velocity model. The desired quantity in the inverse problem, the vector $\Delta\alpha(z)$, contains a set of corrections to the current model that will reduce the size of the residual vector.

In a typical inverse modelling study, the computation of differential seismograms is the major burden, equivalent to the computation of a perturbed synthetic for each layer of the velocity model to be estimated, and one synthetic for the original unperturbed velocity model. When differential seismograms are computed, only a single layer at a time is perturbed, and a difference approximation for the derivative is used, such as

$$\frac{\partial S_{syn}[t, \alpha(z)]}{\partial \alpha(z)} \approx \frac{\{S_{syn}[t, \alpha(z) + \delta\alpha(z)] - S_{syn}[t, \alpha(z)]\}}{\delta\alpha(z)} \tag{10}$$

where $\delta\alpha(z)$ represents the perturbed parameter in the velocity model.

Differential seismograms can be efficiently computed by carefully considering which parts of the computation are changed by the perturbation of any particular layer. In the synthesis integrals, eqs (1z), (1r), and (1t), the dependence of the velocity model is completely contained in the functions $u_z(p, m, \omega)$, $u_r(p, m, \omega)$, and $u_t(p, m, \omega)$ describing the response of the model as a function of frequency and slowness. Eq. (2) , defining $u_z(p, m, \omega)$ and $u_r(p, m, \omega)$, and the equivalent scalar equation for $u_t(p, m, \omega)$, depend on the velocity model for the reflection and transmission coefficients at the interface between the layers of the model and the traveltime through the layers in the model. The interface coefficients and the propagation delays are used to recursively calculate the reflection and transmission matrices in eq. (2) which represent the response of portions of the layered region. In addition, the source terms in eq. (2) also depend on the velocity-model

parameters of the source layer which are used to transform the moment-tensor amplitudes into the compressional and shear-wave amplitudes. Eq. (2) makes a division of the model at the source depth with some terms representing the interaction of waves with the model below the source depth and other terms representing the interaction with the model above the source depth.

To calculate a differential seismogram we subdivide the model into regions above or below the perturbed layer. If the perturbed layer is above the source layer, the source term in eq. (2) $\mathbf{v}_U(z_s, \omega, p, m)$, and the reflectivity of the region below the source layer, $\mathbf{R}_D^{SN}$ will be unchanged. If the perturbed layer is below the source layer, the source term will again be unchanged and the reflectivity of the region above the source, $\mathbf{R}_U^{fS}$ and the receiver function term, $\tilde{\mathbf{W}}[\mathbf{I} - \mathbf{R}_D^{0S}\tilde{\mathbf{R}}]^{-1}\mathbf{T}_U^{0S}$ will be unchanged. If the perturbed layer is the source layer, all these terms will be perturbed. Using generalizations of the techniques described in Randall (1989) the perturbations of the terms in eq. (2) can be efficiently computed.

The efficient generation of differential seismograms requires that two direct computations for each of the terms $\mathbf{R}_D^{SN}$, $\mathbf{R}_U^{fS}$ and $\tilde{\mathbf{W}}[\mathbf{I} - \mathbf{R}_D^{0S}\tilde{\mathbf{R}}]^{-1}\mathbf{T}_U^{0S}$ be performed, in effect computing the forward problem twice. One of the direct recursions (called top down) for each term starts at the top layer of the model and computes recursively toward the bottom layer, while saving the intermediate result at each layer which is the response above that layer. For example, for the top down recursion for $\mathbf{R}_U^{fS}$ the intermediate results $\mathbf{R}_U^{f,1}$, $\mathbf{R}_U^{f,2}$, through $\mathbf{R}_U^{f,S-1}$ are saved. The second direct recursion for each term (called bottom up) starts at the bottom layer and computes recursively toward the top layer, saving the intermediate result at each layer which is the response below that layer. For example, the bottom-up recursion computes $\mathbf{R}_D^{S,N}$ while saving intermediate results from $\mathbf{R}_D^{N-1,N}$ through $\mathbf{R}_D^{S-1,N}$ while progressing up through the model. The third required computation is an indirect formulation, centred about an arbitrary layer, which computes the response for each term using the intermediate response above and below that layer. These intermediate responses are saved as partial results of the direct top-down and bottom-up recursions, and are combined with a reverberation in that layer. The indirect formulation makes it efficient to compute a differential seismogram for a perturbed layer by re-using the computations for the response above and below that perturbed layer, and computing only the terms actually changed by perturbing the layer.

The two direct calculations are merely two different ways to compute the terms of eq. (2) and each have a cost equivalent to a single calculation of the displacement in the (ω, p) domain, with a modest overhead to save the results at each layer. The indirect calculation requires a computation nearly equivalent to adding a single layer in either of the first two algorithms, but the third algorithm is executed once for each layer perturbed, and so is roughly equivalent to the computation required for a single calculation of either of the two forward problems.

Thus, in the time it takes to compute the integrand for three seismograms, the synthetic seismogram and a differential seismogram for each layer can be computed in the (ω, p) domain. The integrals in eq. (1) must be performed for the each of the differential seismograms as well as the synthetic seismogram. For typical inverse-modelling studies, the velocity model is over-parametrized by many thin layers which are adjusted by the inversion process to match observed data. The over-parametrization allows incorrect initial placement of major structural features, such as the Moho, to be corrected by the inversion. Furthermore, the over-parametrization allows simulation of gradients in the velocity structure. With many layers, the computation of the terms in eq. (2) can form a large part of the total computation required for calculating the synthetic and differential seismograms, dominating the computations required for the integrations in eq. (1). In this case the efficient computation of the synthetic and differential seismograms will be nearly equivalent to the time required to compute three synthetic seismograms. The simple brute-force approach would require a time proportional to the computation of $N+1$ synthetic seismograms for an N-layered model. For $N = 30$, the ratio of efficient to brute force will be 3/31 so approximately 90 per cent savings can be realized. Larger numbers of layers will result in larger saving. Since the cost of synthetic seismograms for complete waveforms in layered media is substantial, this saving can make waveform modelling with inverse methods substantially more attractive.

4 ALGORITHMS FOR EFFICIENT DIFFERENTIAL SEISMOGRAMS

The general discussion of the technique above divides the computation of differential seismograms into three distinct cases. In the first case, the perturbed layer is above the source layer, in the second case the perturbed layer is below the source layer, and in the third case the perturbed layer is the source layer. Although the three cases are different there is actually a great deal of similarity in the solution methods. For the discussion below, we define interface 0 as the free surface, interface L-1 as the top layer L, and interface L as the bottom of layer L. The reflection and transmission matrices have superscripts which correspond to the top and bottom layers of the region the matrices represent. If the superscripts differ by exactly one, the matrix corresponds to an interface, and if this difference is greater than one, the matrix represents the response of a layered region. Interface matrices are functions of the earth model and the slowness, but are independent of frequency.

4.1 Perturbation to a layer above the source

If the perturbed layer is above the source layer, both the receiver function, $\tilde{\mathbf{W}}[\mathbf{I} - \mathbf{R}_D^{0S}\tilde{\mathbf{R}}]^{-1}\mathbf{T}_U^{0S}$, and the reflectivity of the region above the source, $\mathbf{R}_U^{fS}$, must be efficiently computed. Both of these terms share the same interface matrices and propagation delays, similar iternal reverberation operators and can be synthesized jointly to avoid duplicate computations. The details of the efficient computation of the receiver function for perturbations is contained in (Randall 1989) and will not be reviewed here.

The top-down recursion for $\mathbf{R}_U^{fS}$ is initialized by setting the reflectivity to the free-surface reflection operator $\tilde{\mathbf{R}}$ and then

successively adding deeper layers with the recursion

$$\mathbf{R}_{\mathrm{U}}^{fL} = \mathbf{R}_{\mathrm{U}}^{L-1,L} + \mathbf{T}_{\mathrm{D}}^{L-1,L}\mathbf{P}^{L-1}\mathbf{R}_{\mathrm{U}}^{f,L-1} \times [\mathbf{I} - \mathbf{P}^{L-1}\mathbf{R}_{\mathrm{D}}^{L-1,L}\mathbf{P}^{L-1}\mathbf{R}_{\mathrm{U}}^{f,L-1}]^{-1}\mathbf{P}^{L-1}\mathbf{T}_{\mathrm{U}}^{L-1,L} \quad (11)$$

which adds layer L to $\mathbf{R}_{\mathrm{U}}^{f,L-1}$, the reflectivity for the region from layer $L-1$ to the free surface. This corrects an error in eq. (7) of Randall (1989) by including the term $\mathbf{R}_{\mathrm{U}}^{L-1,L}$ which is the reflection from the interface between layers L and $L-1$. The vertical propagation delay matrix, $\mathbf{P}^{L-1}$, is a diagonal matrix containing the phase delays in terms of the vertical slowness

$$\mathbf{P}^{L-1} = \begin{pmatrix} \exp(i\omega h\sqrt{\alpha^{-2} - p^2}) & 0 \\ 0 & \exp(i\omega h(\sqrt{\beta^{-2} - p^2})) \end{pmatrix}, \quad (12)$$

for the compressional (α) and shear (β) wave velocities and thickness (h) in layer $L-1$ for horizontal slowness p. After recursion, layer L now forms the new 'bottom' layer. The calculation is continued downward until the source layer is added ($L = S$) yielding $\mathbf{R}_{\mathrm{U}}^{fS}$. For each layer, the value of $\mathbf{P}^{L-1}\mathbf{R}_{\mathrm{U}}^{f,L-1}\mathbf{P}^{L-1}$ is saved for use in efficiently generating the response for a perturbation in layer L.

For the bottom-up recursion, three separate recursions are initialized with $\mathbf{R}_{\mathrm{U}}^{S-1,S}$, $\mathbf{R}_{\mathrm{D}}^{S-1,S}$ and $\mathbf{T}_{\mathrm{U}}^{S-1,S}$, the interface matrices for the top of the source layer. The bottom-up recursion for $\mathbf{R}_{\mathrm{D}}^{L,S}$ and $\mathbf{T}_{\mathrm{U}}^{L,S}$ for the region bounded above the layer L and below by layer S are presented in Randall (1989). The bottom recursion for $\mathbf{R}_{\mathrm{U}}^{L,S}$ is

$$\mathbf{R}_{\mathrm{U}}^{L,S} = \mathbf{R}_{\mathrm{U}}^{L+1,S} + \mathbf{T}_{\mathrm{D}}^{L+1,S}\mathbf{P}^{L+1}\mathbf{R}_{\mathrm{U}}^{L,L+1} \times [\mathbf{I} - \mathbf{P}^{L+1}\mathbf{R}_{\mathrm{D}}^{L+1,S}\mathbf{P}^{L+1}\mathbf{R}_{\mathrm{U}}^{L,L+1}]^{-1}\mathbf{P}^{L+1}\mathbf{T}_{\mathrm{U}}^{L+1,S}. \quad (13)$$

The partial results for $\mathbf{R}_{\mathrm{U}}^{L+1,S}$, $\mathbf{P}^{L+1}\mathbf{R}_{\mathrm{D}}^{L+1,S}\mathbf{P}^{L+1}$ and $\mathbf{P}^{L+1}\mathbf{T}_{\mathrm{U}}^{L+1,S}$ are saved for the efficient solution. The symmetry relations (Kennett 1983) and the results for transposing matrix products provide a relationship

$$[\mathbf{P}^{L+1}\mathbf{T}_{\mathrm{U}}^{L+1,S}]^T = \mathbf{T}_{\mathrm{D}}^{L+1,S}\mathbf{P}^{L+1} \quad (14)$$

that can be exploited to simplify the computation and reduce storage requirements. The symmetry relations do not hold in general, and depend on the particular normalization schemed used in Kennett (1983) and implemented in this code.

For the final assembly of the seismogram for a perturbation of layer L we first update both the top-down and bottom-up recursions by adding the perturbed interfaces at the top and bottom boundaries of the perturbed layer. Then we combine the partial results with the reverberation for the perturbed layer to form $\mathbf{R}_{\mathrm{U}}^{fS}$ by

$$\mathbf{R}_{\mathrm{U}}^{fS} = \mathbf{R}_{\mathrm{U}}^{L,S} + \mathbf{T}_{\mathrm{D}}^{L,S}\mathbf{P}^{L}\mathbf{R}_{\mathrm{U}}^{fL}\mathbf{P}^{L}[\mathbf{I} - \mathbf{R}_{\mathrm{D}}^{L,S}\mathbf{P}^{L}\mathbf{R}_{\mathrm{U}}^{fL}\mathbf{P}^{L}]^{-1}\mathbf{T}_{\mathrm{U}}^{L,S} \quad (15)$$

using the perturbed phase delay matrix, $\mathbf{P}^{L}$, for layer L.

4.2 Perturbation to a layer below the source

Perturbations to a layer below the source layer will only alter $\mathbf{R}_{\mathrm{D}}^{SN}$ where layer N is the half-space at the bottom of the model. The technique for finding bottom-up and top-down recursions for $\mathbf{R}_{\mathrm{D}}^{SN}$ is analogous to the problem just discussed for $\mathbf{R}_{\mathrm{U}}^{fS}$ and the equations are very similar. The bottom-up recursion is initialized by $\mathbf{R}_{\mathrm{D}}^{N-1,N}$ and has been described in Randall (1989).

The top-down recursions are initialized with $\mathbf{R}_{\mathrm{D}}^{S,S+1}$, $\mathbf{T}_{\mathrm{D}}^{S,S+1}$, and $\mathbf{R}_{\mathrm{U}}^{S,S+1}$ and the recursions add layer L with

$$\mathbf{R}_{\mathrm{D}}^{S,L} = \mathbf{R}_{\mathrm{D}}^{S,L-1} + \mathbf{T}_{\mathrm{U}}^{S,L-1}\mathbf{P}^{L-1}\mathbf{R}_{\mathrm{D}}^{L-1,L}\mathbf{P}^{L-1} \times [\mathbf{I} - \mathbf{R}_{\mathrm{U}}^{S,L-1}\mathbf{P}^{L-1}\mathbf{R}_{\mathrm{D}}^{L-1,L}\mathbf{P}^{L-1}]^{-1}\mathbf{T}_{\mathrm{D}}^{S,L-1} \quad (16)$$

$$\mathbf{T}_{\mathrm{D}}^{S,L} = \mathbf{T}_{\mathrm{D}}^{L,L-1}\mathbf{P}^{L-1}[\mathbf{I} - \mathbf{R}_{\mathrm{U}}^{S,L-1}\mathbf{P}^{L-1}\mathbf{R}_{\mathrm{D}}^{L-1,L}\mathbf{P}^{L-1}]^{-1}\mathbf{T}_{\mathrm{D}}^{S,L-1} \quad (17)$$

$$\mathbf{R}_{\mathrm{U}}^{S,L} = \mathbf{R}_{\mathrm{U}}^{L-1,L} + \mathbf{T}_{\mathrm{D}}^{L,L-1}\mathbf{P}^{L-1}\mathbf{R}_{\mathrm{U}}^{S,L-1}\mathbf{P}^{L-1} \times [\mathbf{I} - \mathbf{R}_{\mathrm{D}}^{L,L-1}\mathbf{P}^{L-1}\mathbf{R}_{\mathrm{U}}^{S,L-1}\mathbf{P}^{L-1}]^{-1}\mathbf{T}_{\mathrm{U}}^{L-1,L} \quad (18)$$

again exploiting the transpose relationship for the transmission matrices for efficiency in both computation and storage of intermediate results.

Again the final assembly of the seismogram for a perturbation of layer L begins with updates to both the top-down and bottom-up recursions to include the interfaces at the top and bottom boundaries of the perturbed layer. Then these partial results are combined with the reverberation for the perturbed layer to form $\mathbf{R}_{\mathrm{D}}^{SN}$ by

$$\mathbf{R}_{\mathrm{D}}^{SN} = \mathbf{R}_{\mathrm{D}}^{SL} + \mathbf{T}_{\mathrm{U}}^{S,L}\mathbf{P}^{L}\mathbf{R}_{\mathrm{D}}^{L,N}\mathbf{P}^{L}[\mathbf{I} - \mathbf{R}_{\mathrm{U}}^{S,L}\mathbf{P}^{L}\mathbf{R}_{\mathrm{D}}^{L,N}\mathbf{P}^{L}]^{-1}\mathbf{T}_{\mathrm{D}}^{L,S} \quad (19)$$

completing the calculation for the perturbed model.

4.3 Perturbation in the source layer

A perturbation of the source layer is easily handled by first using the top-down recursion for $\mathbf{R}_{\mathrm{U}}^{fS}$ and the receiver function, and the bottom-up recursion for $\mathbf{R}_{\mathrm{D}}^{SN}$ to add the perturbed interfaces at the top and bottom of the source layer respectively. Then a set of modified source terms, $\Sigma_{\mathrm{U}}(z_s, \omega, p, m)$ and $\Sigma_{\mathrm{D}}(z_s, \omega, p, m)$ must be calculated based on the perturbed velocity model using the eqs 4.59, 4.60 and 4.63 in Kennett (1983), which transform the moment-tensor amplitudes into compressional and shear-wave amplitudes.

At this point all the terms for a perturbation of any layer in the model are available, and eq. (2) may be rapidly evaluated for every layer and integrated using eq. (1) to produce a synthetic and N differential seismograms.

5 DISCUSSION AND CONCLUSIONS

The code which computes the synthetic seismograms was developed and results compared with a standard reflectivity code (Müller 1985) to validate the code for a variety of earth models and source mechanisms. After establishing that the synthetic seismogram code was performing correctly, we made the modifications described here to efficiently calculate differential seismograms in layered media. Differential seismograms were computed first by brute force using the synthetic code for a velocity structure, and then for perturbed velocity structures, with a single perturbation in a layer, computing $N+1$ synthetic seismograms and forming the finite-difference approximation to the differential seismogram as described in eq. (10) above. The efficient-differential-seismogram technique was then used to generate differential seismograms for the same set of model perturbations.

Comparison of the differential seismograms produced by the efficient and brute-force techniques showed no significant differences. The differences between the results of the two techniques were sufficiently small that they are doubtless due to the finite-precision floating-point arithmetic and the difference between the brute-force and efficient-differential-seismogram algorithms.

For demonstration purposes we have calculated the differential seismograms for model M45 (Romanowicz 1982) for Tibet shown in Fig. 1. This is a model appropriate for surface-wave studies with thick layers which would be subdivided into thinner layers for inverse modelling regional seismograms. Here we present the results for the original model with thick layers. The source is a simple, but unrealistic, moment tensor *Mzz* of 10^{20} dyne cm at 10 km depth with a Heaviside-step source–time function. The synthetic-displacement seismogram vertical component is displayed in Fig. 2 for a distance of 300 km from the source. The differential seismograms for perturbations of the shear and compressional velocities are displayed in Fig. 3(a) and (b) respectively with each trace displayed at full scale to show the details of the waveforms. In Figs 4(a) and (b) these differential seismograms are displayed with each group of differential seismograms on a common scale for that group, demonstrating the relative sensitivities of the layers. The regional surface waves show a strong sensitivity to the structure at shallow depths for both compressional and shear-wave perturbations. The differential seismograms for the deeper structure show that the sensitivity of the compressional and shear-wave portions of the seismogram depend predominantly on the corresponding velocity structure. These figures do not display other important sensitivities such as the source mechanism and depth which will influence the relative amplitude of body and surfaces waves by the source excitation. Clearly in an inversion for structure the source depth and mechanism must be accurately estimated first (Wallace, Helmberger & Mellman 1981) using techniques that are relatively insensitive to the details of the velocity structure.

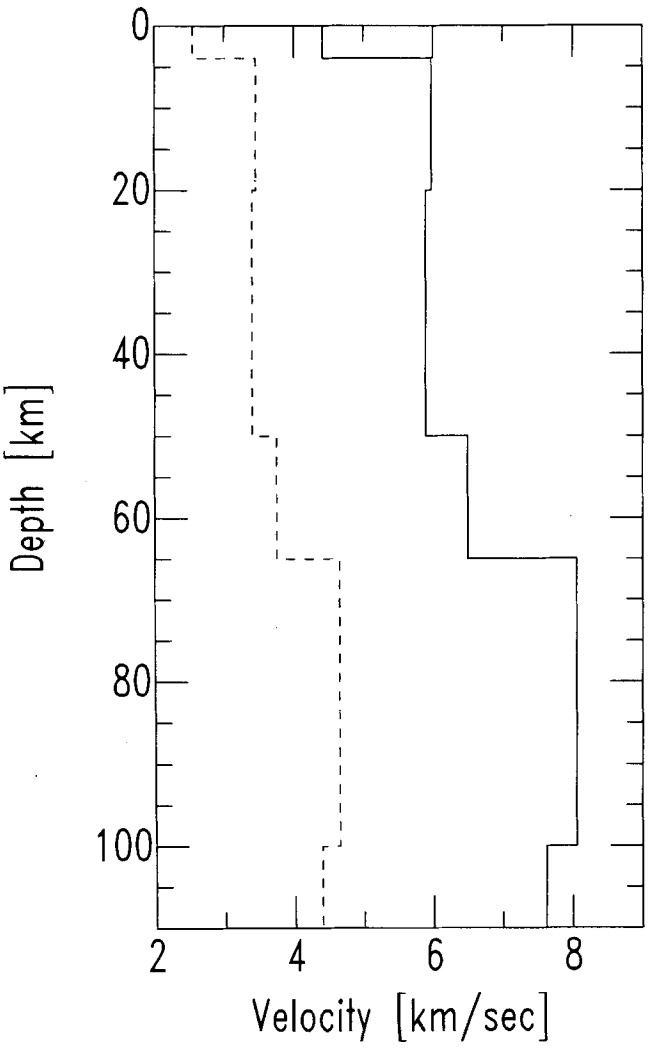

Figure 1. Velocity model M45 for Tibet (Romanowicz 1982) with compressional velocities derived from shear velocities using Poisson's ratio of 0.25.

Efficiency considerations dictate the structure of the computation (Phinney, Odom & Fryer 1987) in several ways. The frequency independence of the interface reflection and transmission coefficients dictates that the computation for all frequencies be done before changing the slowness. This permits a single computation of the interface coefficients at a given slowness to be used in the recursive matrix calculations for all frequencies. Since each slowness calculation is independent, a logical division for massively parallel processors is to assign a portion of the total slowness integral to each available processor. Each processor solves eq. (2) and integrates eq. (1) over its assigned slowness range for all frequencies. Next, the results from all the processors are combined to complete the slowness integration. Finally, the remaining function is inverse Fourier transformed to produce the temporal response. The additional consideration of whether the matrix recursions are done for a single frequency over all the layers, or over all frequencies before adding the next layer will depend on the availability of vector processing hardware and compiler support.

Storage of the unperturbed, frequency-independent interface transmission and reflection coefficients for a single slowness is required for the synthetic. An additional quantity of storage is required for the perturbed interface coefficients. For each interface, a 2 by 2 complex matrix requires 32 bytes of storage. At each interface, two reflection and one transmission matrices must be stored as well as the same number of perturbed matrices for perturbations both above and below the interface. For N layers this is $576N$ bytes or 28800 bytes for 50 layers.

Additional storage is required to hold the intermediate results from the top-down and bottom-up recursions which must be saved for the efficient reassembly for each perturbed layer. In a non-vectorized code the storage is allocated for a single frequency and the synthetic and differential seismograms are all calculated before progressing to the next frequency. In a vectorized code the intermediate results grow by a factor of the number of frequencies. For the non-vectorized case, the storage is comparable to the storage required for the interface coefficients.

In most cases the number of frequency values computed

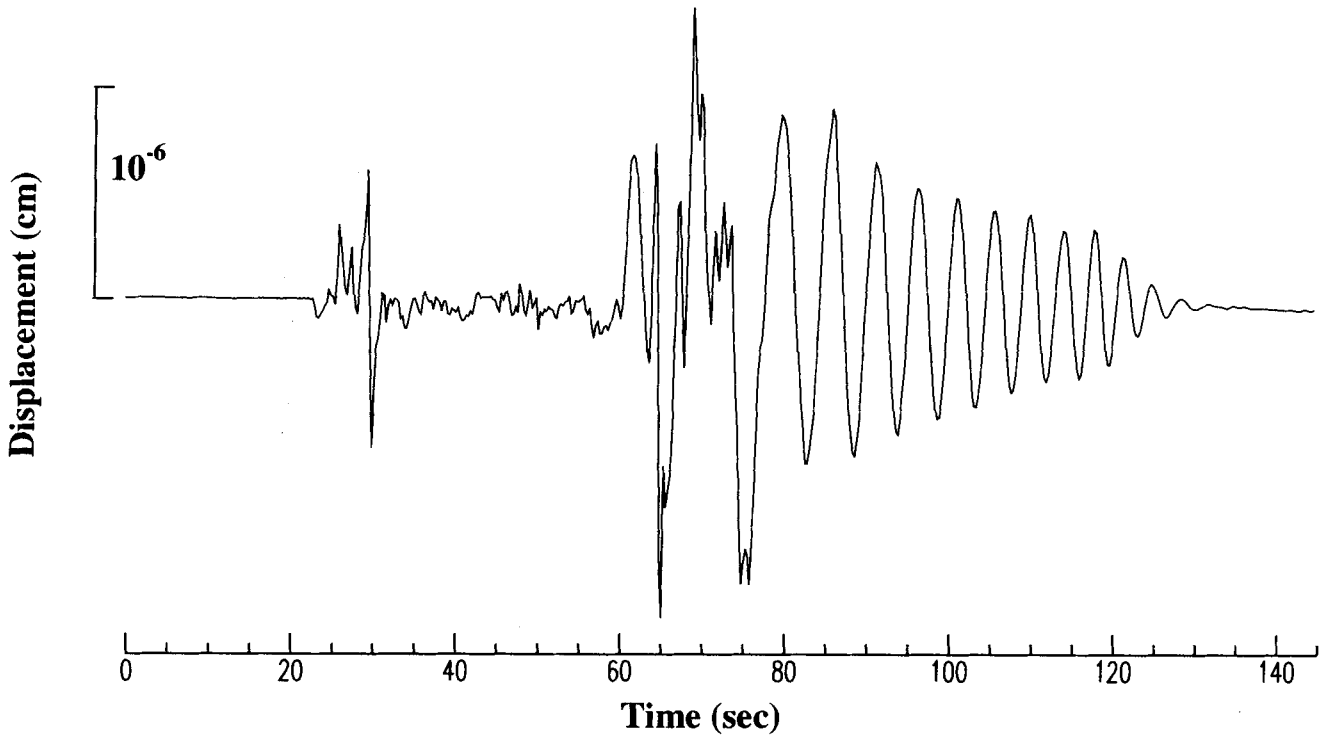

Figure 2. Vertical component of a synthetic displacement seismogram at 300 km from a source at 10 k depth.

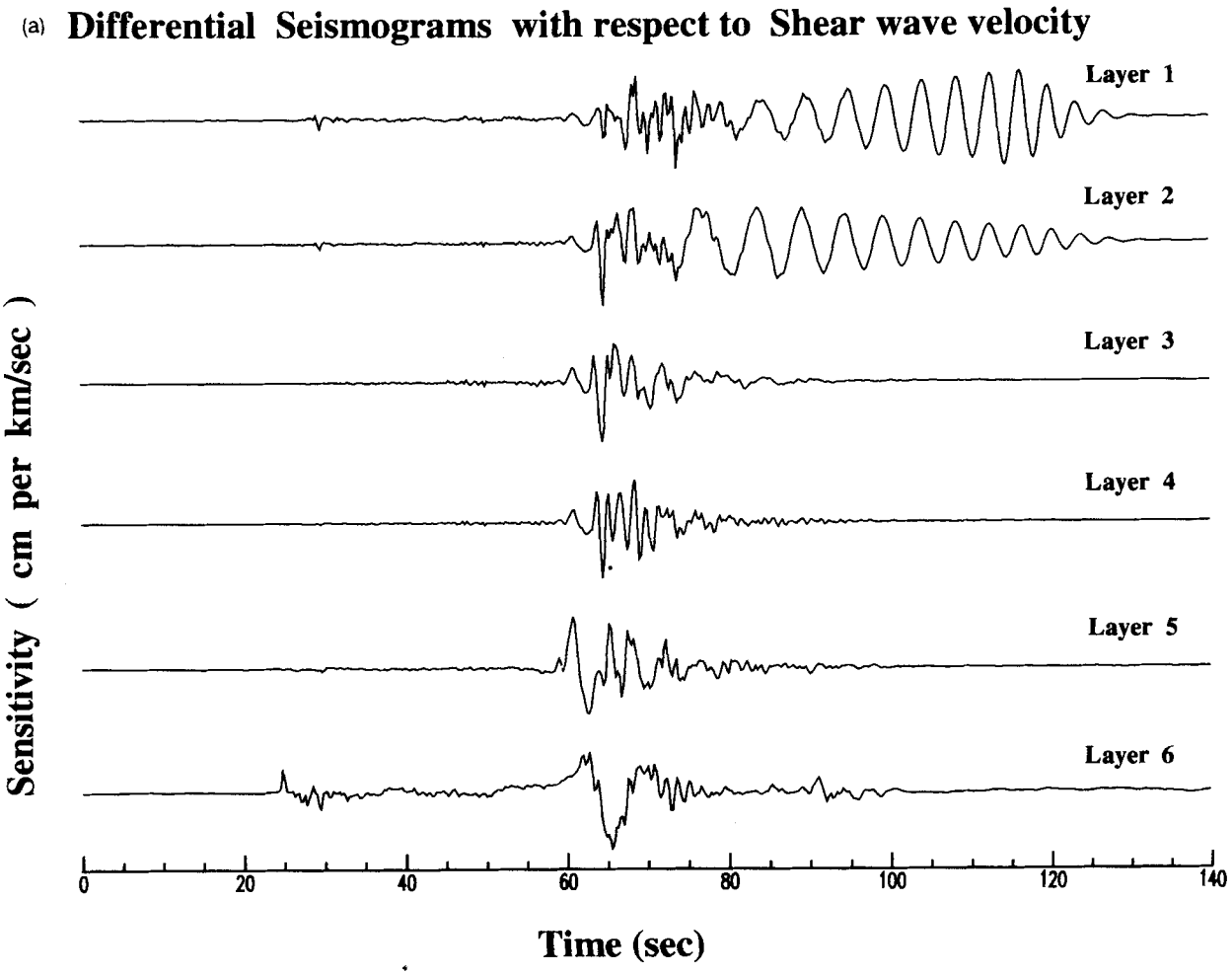

Figure 3. Differential seismograms (vertical components) showing the sensitivities for each layer to shear waves in part (a) and compressional waves in part (b). Each trace is displayed at full scale to show the details of the waveform.

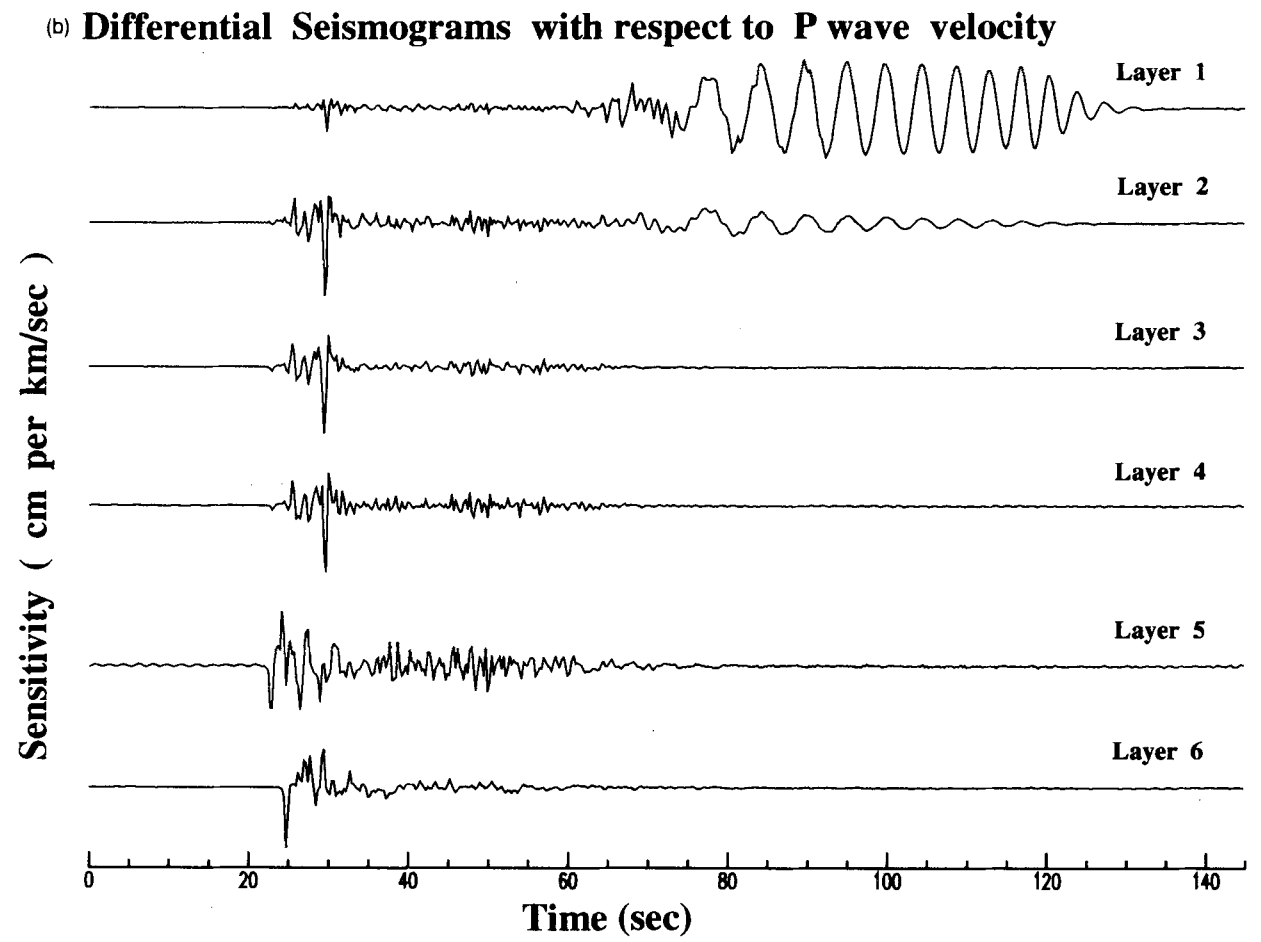

Figure 3. (*Continued.*)

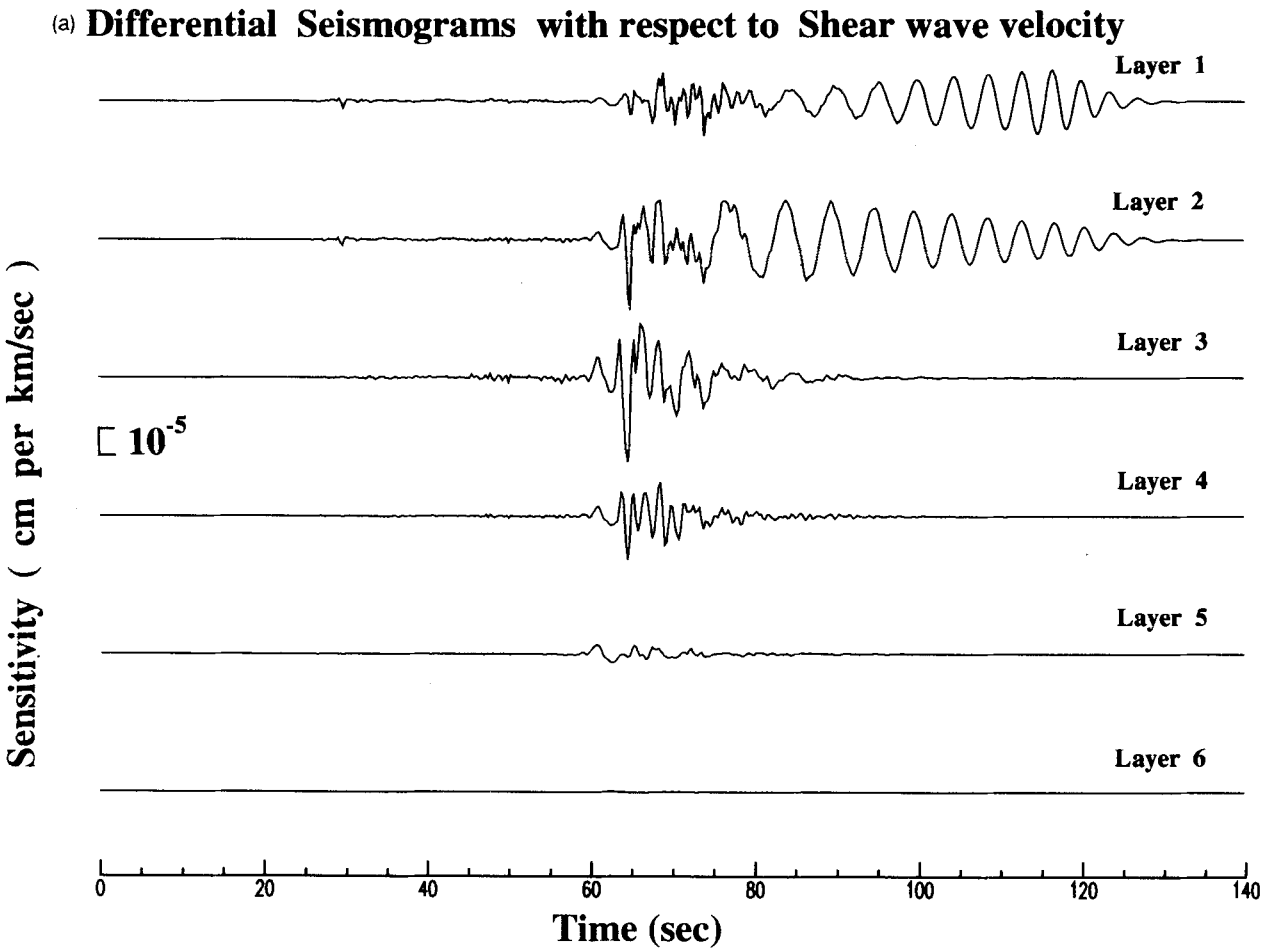

Figure 4. The same differential seismograms as in Fig. 2, but plotted on common scales for shear and compressional waves showing the relat importance of the layers.

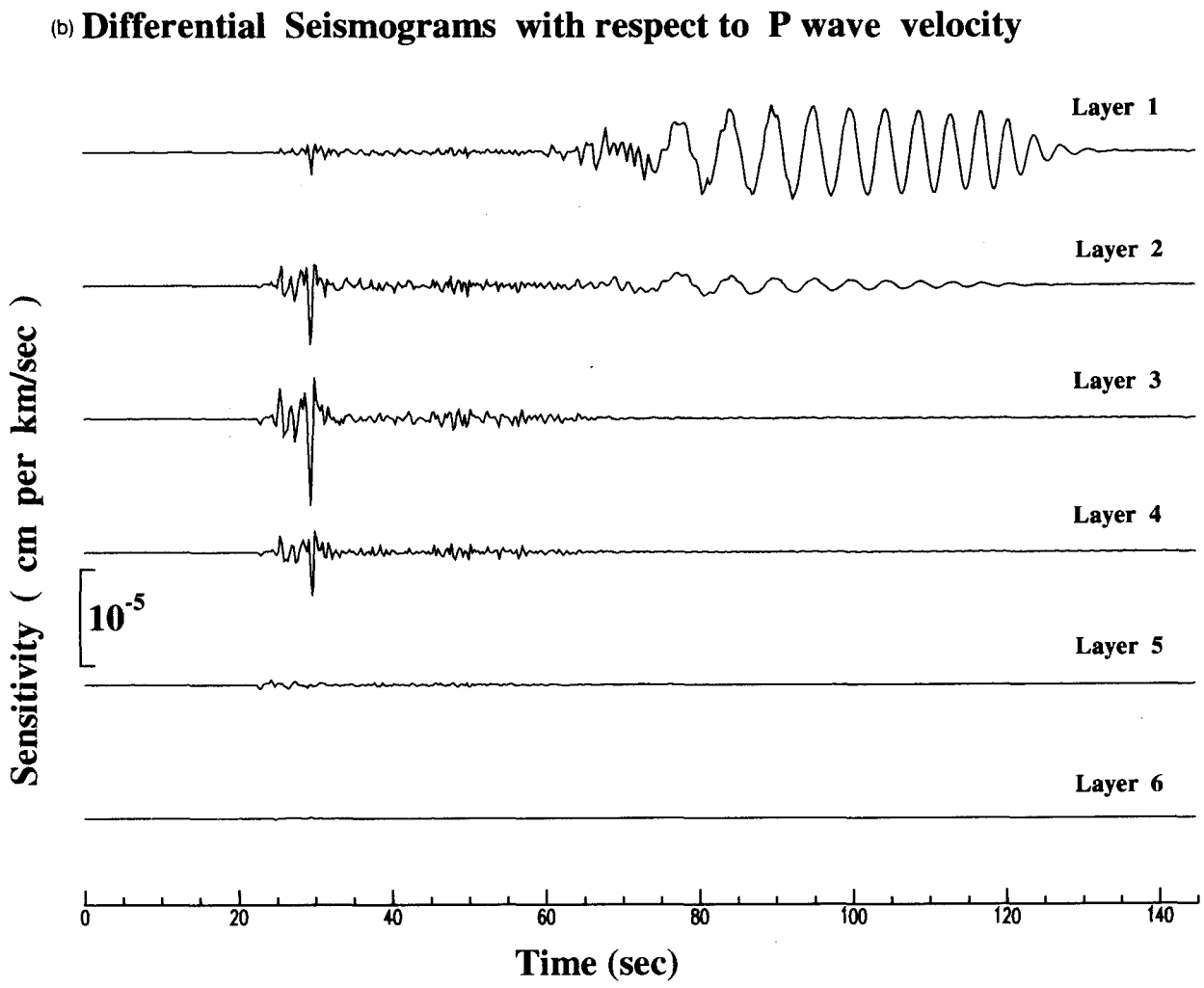

Figure 4. (*Continued.*)

will be larger than the number of layers in the velocity model. The storage required for an N-layer model will be dominated by the arrays for the spectra of the synthetic and N differential seismograms at N_f frequency points. For example, N_f of 1024 and N for 50 layers would require 51 waveforms of 8* 1024 bytes of complex storage, or nearly 0.5 megabytes for every distance modelled.

Computation of complete synthetic seismograms have previously required large mainframe or supercomputers. The rapid growth of both processing speed and available random-access high-speed semi-conductor memory in workstations has made it possible to compute complete synthetic seismograms for many problems with modest hardware. The development of an efficient algorithm for computation of differential seismograms will permit the techniques of inverse theory to be applied to modelling of complete seismograms. As workstation power and size continue to grow, algorithms such as those described here will be required to fully utilize the wealth of broad-band digital data available from the growing number of permanent digital stations and the temporary deployments of portable broad-band seismometers with digital recorders.

ACKNOWLEDGMENTS

Thanks to Chuck Ammon and Harley Benz for the continuing encouragement that led me to undertake this project, and to Chuck Ammon for suggesting changes which significantly improved this paper. Thanks to Steve Taylor for initiating funding from LLNL for the development of the code to compute the complete synthetics which forms the basis of the code described here, and his continuing interest and enthusiasm. Thanks to the Department of Geological Sciences of the University of South Carolina for providing the funding to concentrate on this project as a basis for future work. And Thanks to Tom Owens for creating a geophysics computing facility and an atmosphere conducive to computationally challenging work.

REFERENCES

Backus, G. & Gilbert, F., 1967. Numerical applications of a formalism for geophysical inverse problems, *Geophys. J. R. astr. Soc.*, **13**, 247–276.

Backus, G. & Gilbert, F., 1968. The resolving power of gross earth data, *Geophys. J. R. astr. Soc.*, **16,** 169–205.

Chapman, C.H. & Orcutt, J.A., 1985. The computation of body wave synthtetic seismograms in laterally homogeneous media, *Rev. Geophys.*, **23,** 105–163.

Day, S.M., McLaughlin, K.L., Shkoller, B. & Stevens, J.L., 1989. Potential errors in locked mode synthetics for anelastic earth models, *Geophys. Res. Lett.*, **16,** 203–206.

Franklin, J.N., 1970. Well posed stochastic extensions of ill posed linear problems, *J. Math. Anal. Applic.*, **31,** 682–716.

Fuchs, K. & Muller, G., 1971. Computation of synthetic seismograms with the reflectivity method and comparison with observation, *Geophys. J. R. astr. Soc.*, **23,** 417–433.

Gomberg, J.S. & Masters, T.G., 1988. Waveform modelling using locked-mode synthetic and differential seismograms: application to determination of the structure of Mexico, *Geophys. J.*, **94,** 193–218.

Helmberger, D.V., 1968. The crust–mantle transition in the Bering Sea, *Bull. seism. Soc. Am.*, **58,** 179–214.

Jackson, D.D., 1972. Interpretation of inaccurate, insufficient and inconsistent data, *Geophys. J. R. astr. Soc.*, **28,** 97–110.

Kennett, B.L.N., 1974. Reflections, rays and reverberations, *Bull. seism. Soc. AM.*, **64,** 1685–1696.

Kennett, B.L.N., 1980. Seismic waves in a stratified half space—II. Theoretical seismograms, *Geophys. J. R. astr. Soc.*, **61,** 1–10.

Kennett, B.L.N., 1983. *Seismic Wave Propagation in Stratified Media*, Cambridge University Press, Cambridge.

Kennett, B.L.N. & Kerry, N.J., 1979. Seismic waves in a stratified half space, *Geophys. J. R. astr. Soc.*, **57,** 557–583.

Mallick, S. & Frazer, L.N., 1987. Practical aspects of reflectivity modeling, *Geophysics*, **52,** 1355–1364.

Mellman, G.R., 1980. A method of body-waveform inversion for the determination of earth structure, *Geophys. J. R. astr. Soc.*, **62,** 481–504.

Müller, G., 1985. The reflectivity method: a tutorial, *J. Geophys.*, **58,** 153–174.

Phinney, R.A., Odom, R.I. & Fryer, G.J., 1987. Rapid generation of synthetic seismograms in layered media by vectorization of the algorithm, *Bull. seism. Soc. Am.*, **77,** 2218–2226.

Randall, G.E., 1989. Efficient calculation of differential seismograms for lithospheric receiver functions, *Geophys. J. Int.*, **99,** 469–481.

Romanowicz, B.A., 1982. Constraints on the structure of the Tibet Plateau from pure path phase velocities of Love and Rayleigh waves, *J. geophys. Res.*, **87,** 6865–6883.

Shaw, P.R. & Orcutt, J.A., 1985. Waveform inversion of seismic refraction data and applications to young Pacific crust, *Geophys. J. R. astr. Soc.*, **82,** 375–414.

Wallace, T.C., Helmberger, D.V. & Mellman, G.R., 1981. A technique for the inversion of regional data in source parameter studies, *J. geophys. Res.*, **86,** 1679–1685.